Supporting Information

Shamrock-shaped non-fullerene acceptors via side-chain and end-group engineering for high-efficiency and high-voltage organic photovoltaics

Yi Luo[1], Yunhao Hou[1], Mengwei Ji[1], Sheng Ge[1], Zongtao Wang[2], Mengzhen Du[2], Qing Guo[1], Erjun Zhou[2]**

[1] *School of Materials Science and Engineering, Zhengzhou University, Zhengzhou 450001, China.*

[2] *College of Biological and Chemical Engineering, Jiaxing University, Jiaxing, 314001, China.*

Email: wangzt@zjxu.edu.cn; zhouej@nanoctr.cn

Materials and Synthesis

All materials except AQI81, AQI82 and AQI84 are purchased from commercial companies.

Synthesis of AQI81, AQI82 and AQI84

All the related materials and reagents were purchased from commercial companies and used without further purifications. Compound 2 were synthesized according to the literature.[1]

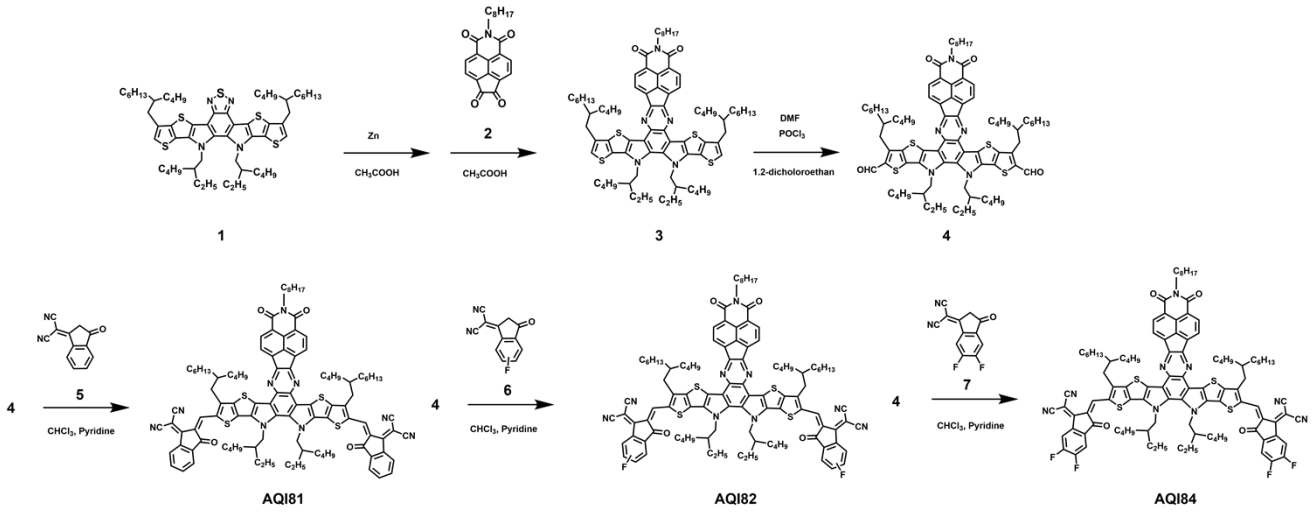

Scheme S1. The synthetic routes of AQI81, AQI82 and AQI84.

Synthesis of compound 3: Under nitrogen protection, zinc powder (490 mg, 4.5 mmol) was added in the solution of compound 1 (500 mg, 0.3 mmol) in acetic acid (25 mL). Then the mixture solution was heated to 80°C and stirred for overnight. After the solution was cooled to room temperature, the

solid was removed by filtration. Transfer the filtrate to a two-neck flask containing compound 2 (97 mg, 0.27 mmol), then the mixture solution was heated to 60°C for 6 h. After cooling to room temperature, washed with saturated salt water and dichloromethane. The solvent was removed under reduced pressure. The crude product was subsequently purified by column chromatography on silica gel to afford compound 3 as green solid (259 mg, 74% yield). ^{1}H NMR (400 MHz, $CDCl_3$) δ 8.65 (d, J = 7.3 Hz, 2H), 8.53 (d, J = 7.3 Hz, 2H), 7.03 (s, 2H), 4.69 (s, 4H), 4.21 (t, J = 7.7 Hz, 2H), 2.82 (s, 4H), 2.19 – 1.96 (m, 4H), 1.77 (p, J = 7.7 Hz, 2H), 1.38 (d, J = 41.2 Hz, 45H), 0.89 (s, 30H), 0.66 (d, J = 26.6 Hz, 12H).

Synthesis of compound 4: Under the protection of nitrogen, 2 mL DMF was added into the two-neck flask. Then, $POCl_3$ (0.1 mL, 1.9 mmol) was injected at 0°C. After being stirred at 0°C for 1 h, the mixture of compound 3 (259 mg, 0.19 mmol) and 1, 2-dichloroethane (5 mL) was directly injected into the two-neck flask. Next, the mixture was stirred at room temperature for overnight, then was cooled to 0 °C (50 mL), neutralized with aqueous $NaHCO_3$ for another 4 h. Washed with $NaHCO_3$ aqueous solution and dichloromethane. The solvent was removed under reduced pressure. The crude product was subsequently purified by column chromatography on silica gel to afford compound 4 as green solid (258 mg, 96% yield). ^{1}H NMR (400 MHz, $CDCl_3$) δ 10.16 (s, 2H), 8.69 (d, J = 7.3 Hz, 2H), 8.56 (d, J = 7.2 Hz, 2H), 4.83 – 4.63 (m, 4H), 4.28 – 4.14 (m, 2H), 3.17 (d, J = 7.3 Hz, 4H), 2.21 – 2.05 (m, 5H), 1.83 – 1.70 (m, 3H), 1.31 (s, 45H), 0.89 (s, 29H), 0.74 – 0.58 (m, 13H).

Synthesis of AQI81: Compound 4 (86 mg, 0.06 mmol) and compound 5 (51 mg, 0.26 mmol) were dissolved into dry chloroform (10 mL) in a two-neck flask. The solution was flushed with nitrogen for 5 min. After 0.3 mL pyridine were added, the mixture was stirred at 65°C overnight. After cooling to room temperature, the reaction mixture was poured into water and extracted several times with chloroform. Then the solvent was removed under reduced pressure, and the crude product was purified by column chromatography on silica gel to yield AQI81 as red solid (85 mg, 78% yield). ^{1}H NMR (400 MHz, $CDCl_3$) δ 9.13 (s, 2H), 8.73 – 8.64 (m, 2H), 8.59 (d, J = 7.2 Hz, 2H), 8.44 (d, J = 7.1 Hz, 2H), 7.96 (dd, J = 6.1, 2.6 Hz, 2H), 7.74 (dd, J = 6.3, 2.8 Hz, 4H), 4.89 (d, J = 8.0 Hz, 4H), 4.17 (t, J = 7.7 Hz, 2H), 3.18 (d, J = 7.6 Hz, 4H), 2.28 (s, 2H), 2.09 (s, 2H), 1.74 (dd, J = 10.9, 4.4 Hz, 2H).

Synthesis of AQI82: Compound 4 (98 mg, 0.07 mmol) and compound 6 (55 mg, 0.24 mmol) were dissolved into dry chloroform (10 mL) in a two-neck flask. The solution was flushed with nitrogen for 5 min. After 0.3 mL pyridine were added, the mixture was stirred at 65°C overnight. After cooling to room temperature, the reaction mixture was poured into water and extracted several times with chloroform. Then the solvent was removed under reduced pressure, and the crude product was purified by column chromatography on silica gel to yield AQI82 as red solid (68 mg, 53% yield). ^{1}H NMR (400 MHz, $CDCl_3$) δ 9.14 (d, *J* = 6.4 Hz, 2H), 8.70 (dd, *J* = 8.7, 4.3 Hz, 1H), 8.63 (d, *J* = 7.2 Hz, 2H), 8.49 (d, *J* = 7.2 Hz, 2H), 8.35 (d, *J* = 10.7 Hz, 1H), 7.96 (dd, *J* = 8.2, 5.2 Hz, 1H), 7.59 (dd, *J* = 6.6, 2.5 Hz, 1H), 7.42 (q, *J* = 8.2 Hz, 2H), 4.87 (s, 4H), 4.26 – 4.11 (m, 2H), 3.19 (d, *J* = 7.9 Hz, 4H), 2.25 (s, 2H), 2.11 (s, 2H), 1.76 (s, 2H), 1.38 (d, *J* = 47.7 Hz, 57H), 0.92 (d, *J* = 17.3 Hz, 24H), 0.72 (d, *J* = 15.0 Hz, 6H).

Synthesis of AQI84: Compound 4 (94 mg, 0.07 mmol) and compound 7 (48 mg, 0.21 mmol) were dissolved into dry chloroform (10 mL) in a two-neck flask. The solution was flushed with nitrogen for 5 min. After 0.3 mL pyridine were added, the mixture was stirred at 65°C overnight. After cooling to room temperature, the reaction mixture was poured into water and extracted several times with chloroform. Then the solvent was removed under reduced pressure, and the crude product was purified by column chromatography on silica gel to yield AQI84 as red solid (63mg, 51% yield). ^{1}H NMR (400 MHz, $CDCl_3$) δ 9.08 (s, 2H), 8.64 (d, *J* = 7.2 Hz, 2H), 8.46 (dd, *J* = 18.6, 6.9 Hz, 4H), 7.69 (t, *J* = 7.5 Hz, 2H), 4.89 (d, *J* = 6.5 Hz, 4H), 4.26 – 4.10 (m, 2H), 3.17 (d, *J* = 7.3 Hz, 4H), 2.37 – 2.23 (m, 2H), 2.15 – 2.01 (m, 2H), 1.75 (dt, *J* = 15.7, 7.3 Hz, 2H), 1.46 – 1.19 (m, 57H), 0.86 (d, *J* = 20.3 Hz, 23H), 0.72 (d, *J* = 9.3 Hz, 6H).

Measurements and characterizations

Materials Characterization

Grazing incidence wide-angle X-ray scattering (GIWAXS) analyses were investigated at the XEUSS SAXS/WAXS equipment. The data were obtained with an area Pilatus 100k detector with a resolution of 195 × 487 pixels (0.172 mm × 0.172 mm). The X-ray wavelength was 1.54 Å, and the incidence angle was 0.2°. The samples were spin-coated onto the Si substrate. AFM was tested by Bruker Dimension Icon Tapping mode. The active layers were spin-coated onto the ITO substrate.

Electrochemical Characterizations

UV-vis spectra were tested by UV-3600i PLUS (Shimadzu Corporation). The film specimens were spin-coated on a quartz substrate. The concentration of solution specimens was 0.01 mg mL^{-1}. Cyclic voltammetry (CV) measurements were carried out using an electrochemical workstation, equipped with a standard three-electrode configuration. Typically, a three-electrode cell equipped with Pt plate coated with a thin film as a working electrode, an Ag/AgCl (0.01 M in anhydrous acetonitrile) reference electrode, and a Pt wire counter electrode was employed. The measurements were done in anhydrous acetonitrile with tetrabutylammonium hexafluorophosphate (0.1 M) as the supporting electrolyte under an argon atmosphere at a scan rate of 100 mV/s. The potential of the Ag/AgCl reference electrode was internally calibrated by using the ferrocene/ferrocenium redox couple (Fc/Fc^{+}). The HOMO and LUMO energy level can be calculated by the equations:

$$E_{HOMO} = - e\ (4.8 + E_{ox} - E^{1/2}_{Fc+/Fc})\ V$$

$$E_{LUMO} = - e\ (4.8 + E_{red} - E^{1/2}_{Fc+/Fc})\ V$$

The *J–V* curves were measured using a Zolix Solar IV-150A-ZZU system. The photocurrent was measured under AM 1.5 G illumination at 100 $mW \cdot cm^{-2}$ using a Zolix HPS-300XA solar simulator. Light intensity was calibrated with a Zolix QE-B1 Si-based solar cell. The EQE spectra were measured using a Zolix SCS10-X150-DSSC-ZZU system.

Photovoltaic device fabrication

The OSCs devices were fabricated with a conventional structure of ITO/PEDOT:PSS/active layer/ PNDIT-F3N/Ag. The ITO-coated glass substrates were sequentially cleaned in detergent deionized water and ethanol for at least 30 min each at room temperature. A thin layer of PEDOT:PSS (30 nm, Heraeus Clevios™ AI 4083) was spin-casted on pre-cleaned ITO-coated glass at 3000 rpm, and then annealed at 150 ℃ for 10 min under ambient atmosphere. The solution for PE4:AQI81 (1:1, w/w, 14 mg mL^{-1} in total), PE4:AQI82 (1:1, w/w, 14 mg mL^{-1} in total), and PE4:AQI84 (1:1, w/w, 14 mg mL^{-1} in total) with was prepared in chloroform and was stirred at 85 ℃ for 2 hours. After cooling down for one minute, the active layers were spin-coated (3000 rpm) from the above solution with thermal annealing of 100 ℃, 10 min. Then, the methanol solution of PNDIT-F3N (1 mg mL^{-1}) was spin-coated on the top of active layer at a speed of 3000 rpm for 30 s. Finally, a 100 nm-thick metal silver electrode was thermally deposited under vacuum conditions of 3×10^{-4} Pa. The active area of

device is 5 mm^2 and mask area is 3.14 mm^2 .

Carrier mobility measurements

Hole-only and electron-only devices were fabricated by using the device structures of ITO/PEDOT:PSS/active layer/Au and ITO/TIPD/active layer/PNDIT-F3N/Ag, respectively. The hole and electron mobilities were approximated by the Mott-Gurney equation: $J = \frac{9}{8}\varepsilon_0\varepsilon_r\mu\frac{V^2}{L^3}$, where J stands for current density, ε_0 is the permittivity of free space (8.85×10−12 $C\cdot V^{-1}\cdot m^{-1}$), ε_r is the relative dielectric constant of the transport medium (assuming that of 3.0), μ is the charge mobility, V is the internal potential in the device, and L is the thickness of the active layer.

Supplementary Figures and Tables

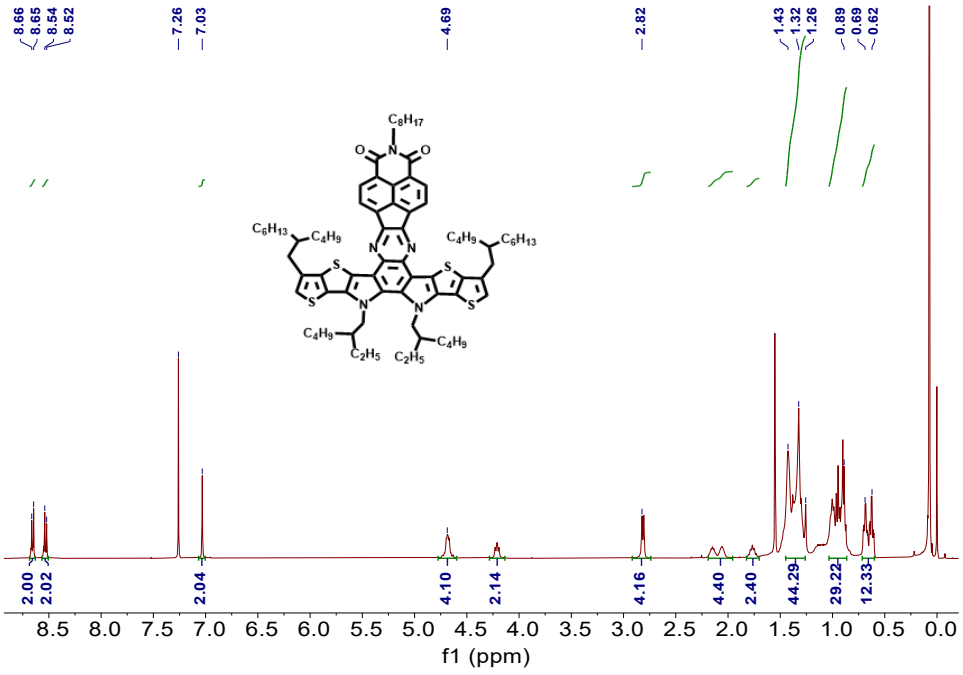

Fig. S1. ^1H NMR spectrum of Compound 3.

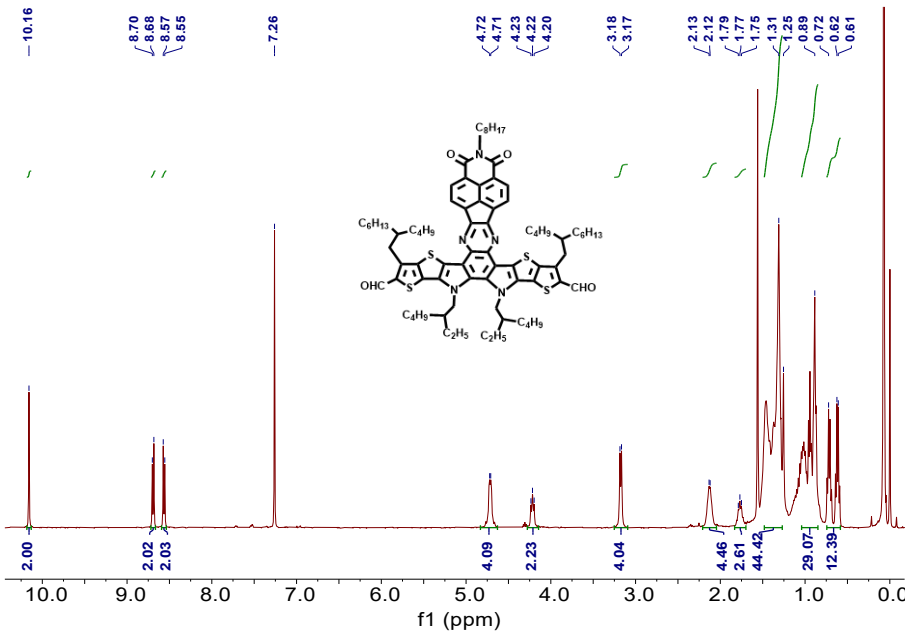

Fig S2. [1]H NMR spectrum of Compound 4.

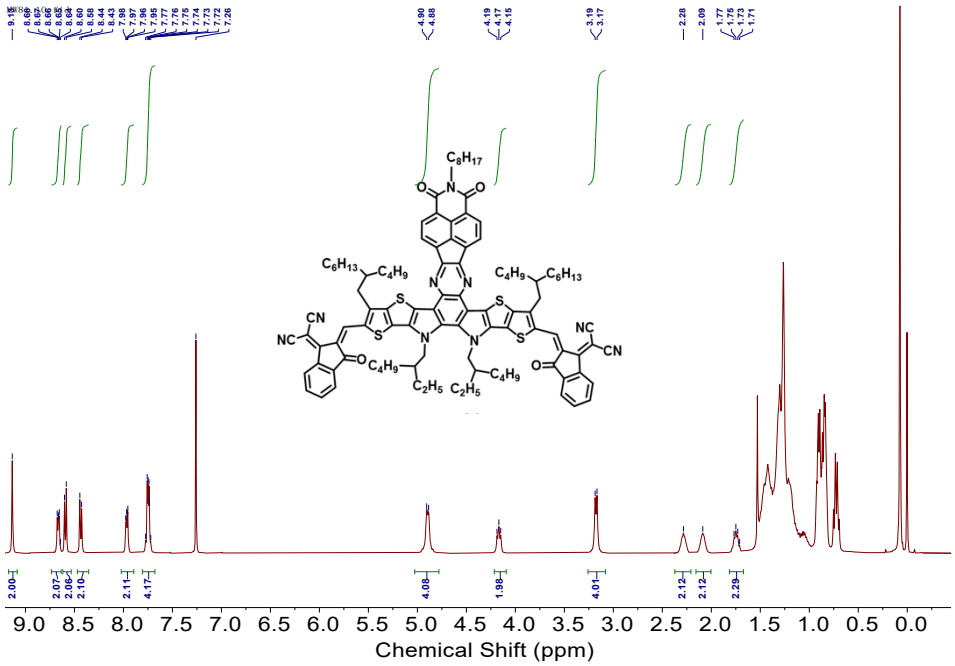

Fig S3. [1]H NMR spectrum of AQI81.

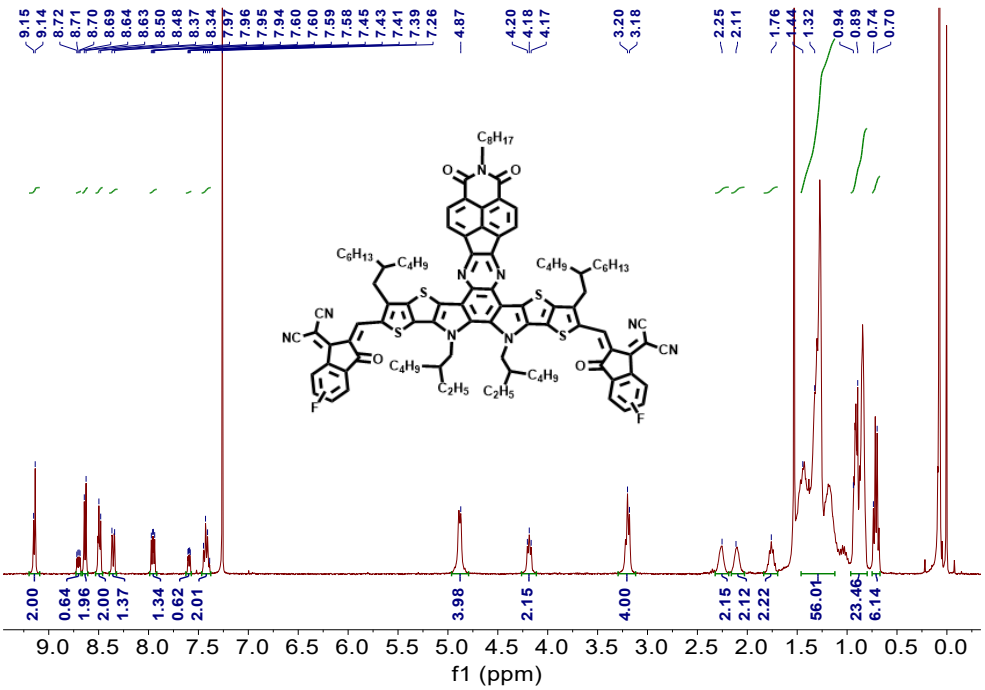

Fig. S4. ^{1}H NMR spectrum of AQI82**.**

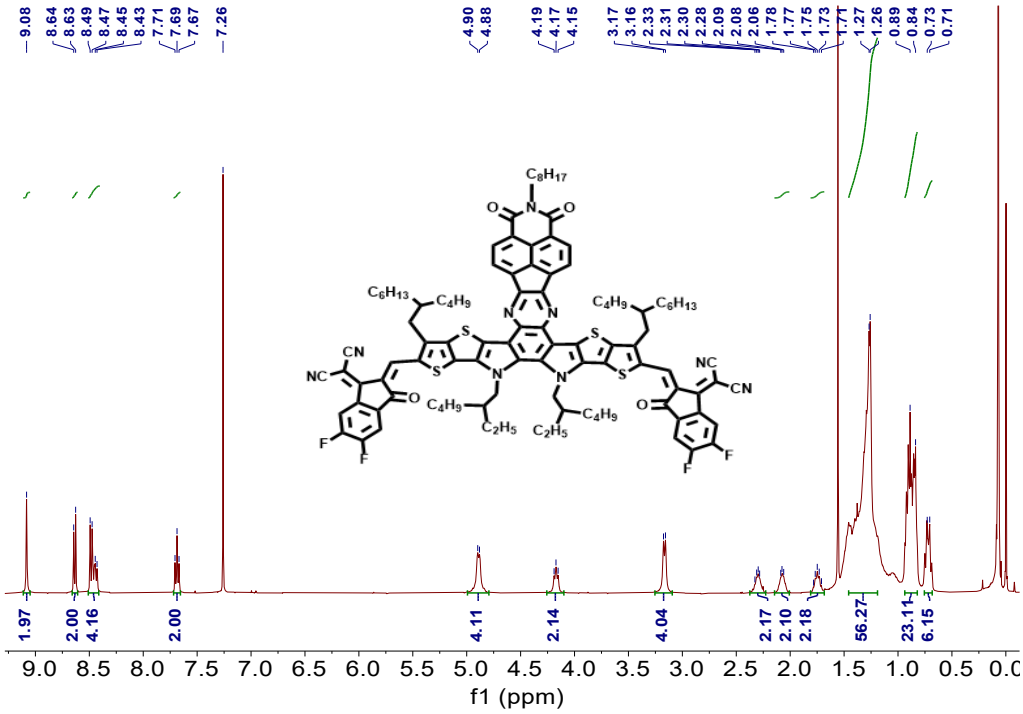

Fig. S5. ^{1}H NMR spectrum of AQI84.

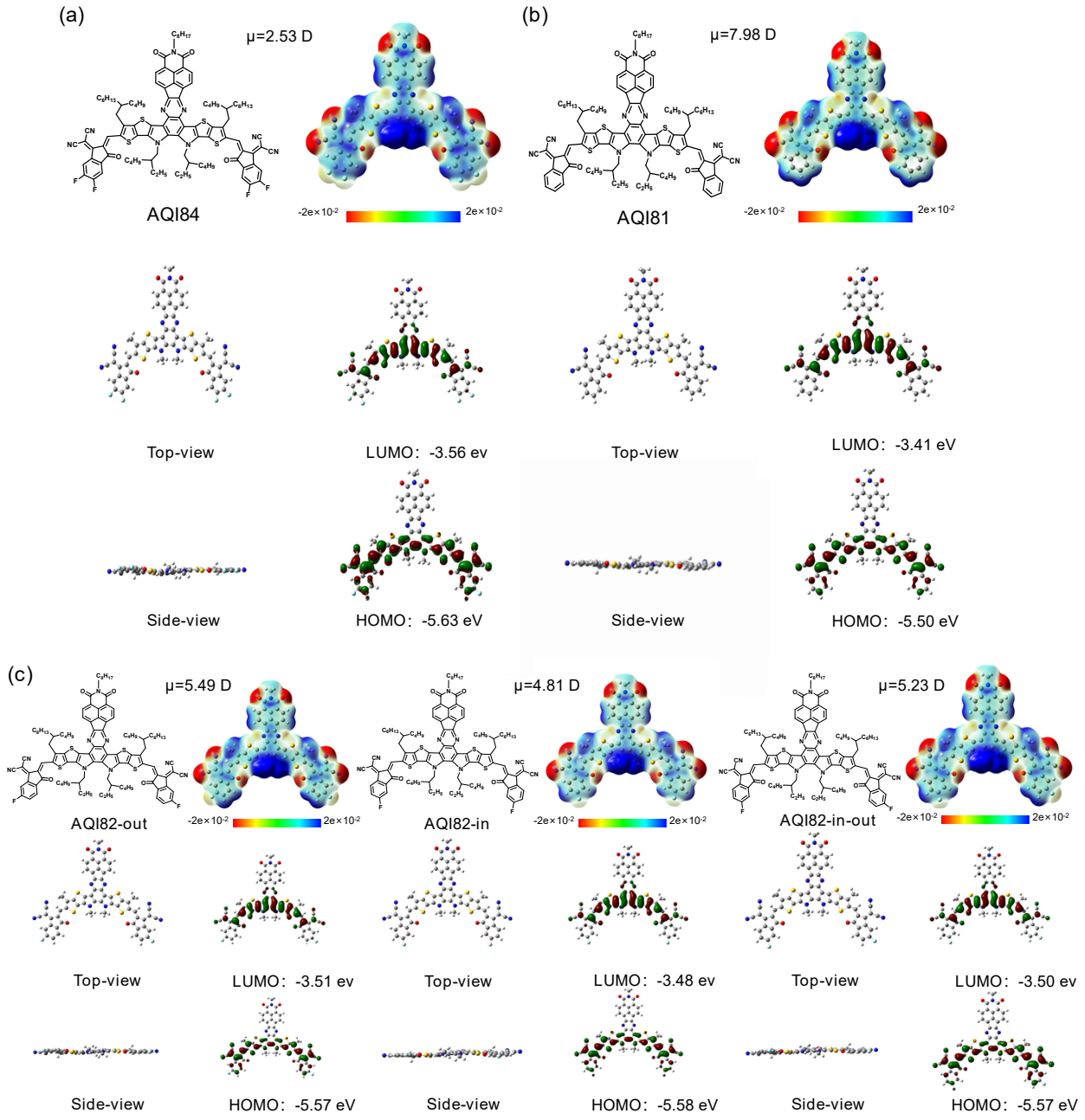

Fig. S6. The side view, top view, molecular orbital energy levels, and molecular electrostatic potential of (a) AQI84, (b) AQI81, and (c) AQI82-out, AQI82-in, and AQI82-in-out.

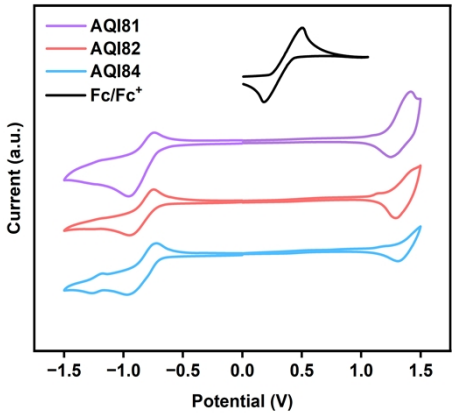

Fig. S7. Cyclic voltammetry curves of AQI81，AQI82 and AQI84.

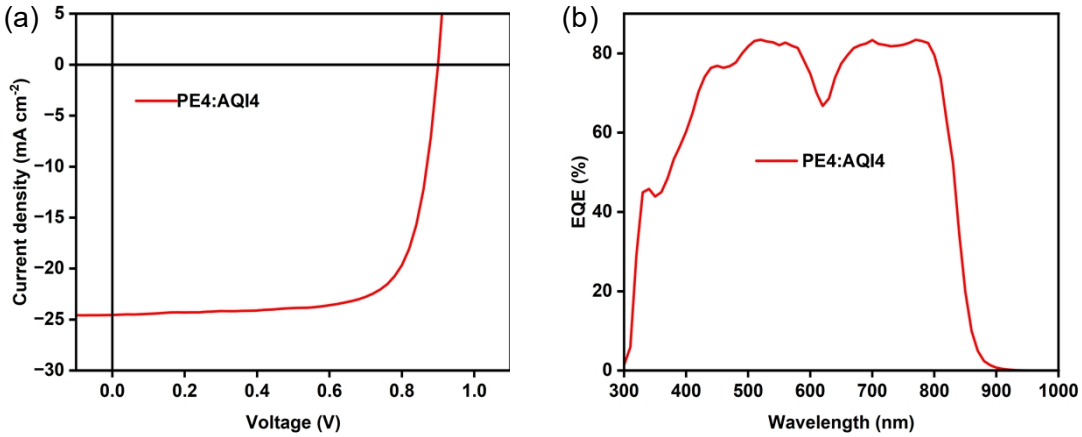

Fig. S8. (a) *J-V* curve of PE4:AQI4. (b) EQE spectrum of PE4:AQI4.

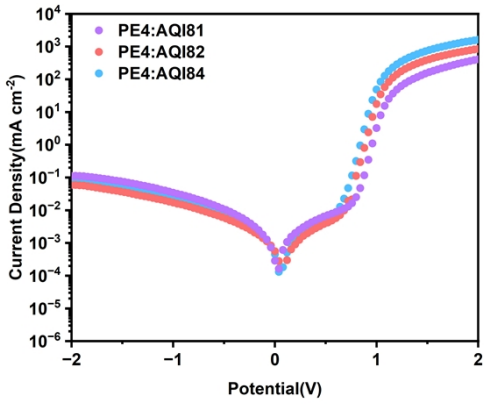

Fig. S9. *J–V* curves under the dark state.

Table S1. Summary of the photophysical and electrochemical properties of PE4, AQI81, AQI82 and AQI84.

Acceptor	$\lambda_{max,}$ sol (nm)	$\lambda_{max,}$ film (nm)	λ_{onset} (nm)	E_{opt}[a] (eV)	HOMO (eV)	LUMO (eV)
AQI81	716	762	827	1.50	-5.58	-3.66
AQI82	724	780	850	1.46	-5.59	-3.68
AQI84	729	787	855	1.45	-5.64	-3.73

[a] Calculation: $E_g^{opt} = 1240/\lambda_{onset}$ (eV).

Table S2. The optimization of additive for PE4:AQI84 (D:A=1:1, TA=100℃).

Compound	V_{OC} (V)	J_{SC} (mA cm^{-2})	FF (%)	PCE (%)
PE4: AQI84 non	0.930	24.07	74.35	16.64
PE4: AQI84 10 mg/ml DIB	0.946	19.72	76.34	14.25
PE4: AQI84 10 mg/ml DBCL	0.935	21.85	76.96	15.74
PE4: AQI84 10 mg/ml DCBB	0.940	20.63	76.04	14.76
PE4: AQI84 10 mg/ml TBB	0.920	20.40	67.76	12.72
PE4: AQI84 0.5% DIO	0.930	20.30	72.66	13.72
PE4: AQI84 0.5% DPE	0.930	21.16	73.54	14.49
PE4: AQI84 0.5% DIM	0.923	22.09	69.97	14.28
PE4: AQI84 0.5% CN	0.926	13.19	69.54	8.51

Table S3. Photovoltaic parameters of the optimized PE4:AQI4 based devices under AM 1.5G illumination, 100 mW cm^{-2}.

Active layer	V_{OC} (V)	J_{SC} (mA cm^{-2})	J_{cal}[a] (mA cm^{-2})	FF (%)	PCE (%)
PE4:AQI4	0.900	24.33	23.11	74.01	16.20

[a] Integrated from EQE curves.

Table S4. G_{max} values of PE4:AQI81, PE4:AQI82, and PE4:AQI84 blend films.

Active layer	G_{max} (10^{28} m^{-3} s^{-1})
PE4:AQI81	1.27
PE4:AQI82	1.43
PE4:AQI84	1.46

Table S5. Charge transport parameters of PE4:AQI81, PE4:AQI82 and PE4:AQI84 based devices.

Active layer	Hole mobility (cm^2 V^{-1} s^{-1})	Electron mobility (cm^2 V^{-1} s^{-1})	μ_h/μ_e
PE4:AQI81	1.95×10^{-4}	1.63×10^{-4}	1.20
PE4:AQI82	2.84×10^{-4}	2.58×10^{-4}	1.10
PE4:AQI84	3.51×10^{-4}	3.20×10^{-4}	1.09

Table S6. Detailed GIWAXS data of PE4:AQI81, PE4:AQI82 and PE4:AQI84 blend films.

Compound	OOP				IP			
	(010)				(100)			
	q (Å^{-1})	*d*-spacing (Å)	FWHM (Å^{-1})	CCL (Å)	*q* (Å^{-1})	*d*-spacing (Å)	FWHM (Å^{-1})	CCL (Å)
PE4: AQI81	1.504	4.179	0.258	22.631	0.275	22.835	0.076	77.396
PE4: AQI82	1.508	4.166	0.244	23.984	0.277	22.670	0.075	77.922
PE4: AQI84	1.513	4.152	0.242	24.182	0.279	22.492	0.074	78.445

References

1. P. Zhou, L. Deng, Z. Han, X. Zhao, Z. Zhang and S. Huo, *RSC Adv.*, 2022, **12**, 13480-13486.